Toxicology Reports 8 (2021) 1087–1097

Contents lists available at ScienceDirect

Toxicology Reports

journal homepage: www.elsevier.com/locate/toxrep

Induction of autophagy has protective roles in imatinib-induced cardiotoxicity

Miyuki Kobara *, Naseratun Nessa, Hiroe Toba, Tetsuo Nakata

Department of Clinical Pharmacology, Division of Pathological Science, Kyoto Pharmaceutical University, Kyoto, Japan

ARTICLE INFO

Edited by Dr. A.M. Tsatsaka

Keywords:
Cardio-oncology
Imatinib
Mitochondria
Autophagy
Apoptosis

ABSTRACT

Cardiotoxicity is one of the severe adverse effects of chemotherapeutic agents. Imatinib was previously reported to induce cardiotoxicity. Autophagy is an intracellular bulk protein and organelle degradation process, but its roles in cardiac diseases are unclear. We examined whether imatinib induces cardiomyocyte autophagy, and the role of autophagy in imatinib-induced cardiotoxicity using *in vitro* and *in vivo* experiments. In *in vitro* experiments, neonatal rat cardiomyocytes were treated with imatinib (1, 5, or 10 μM; 6 h). Myocyte autophagy was assessed by microtubule-associated protein light chain (LC) 3-II, beclin 1, mature cathepsin D, and acridine orange-stained mature autolysosome expression. Imatinib increased their expression, suggesting that it induced autophagy. Consequently, imatinib altered the production of mitochondria-derived reactive oxygen species (ROS) and loss of mitochondrial membrane potential, which were assessed by the fluorescent indicator MitoSOX and JC-1, respectively, leading to cardiomyocyte apoptosis. 3-methyl-adenine (3MA), an autophagic inhibitor, exacerbated imatinib-induced apoptosis by 30 %. In *in vivo* experiments, C57BL/6 mice were treated with imatinib (50 and 200 mg/kg/day) for 5 weeks in the presence or absence of 3MA. Echocardiographic measurement revealed that imatinib (200 mg) caused dilatation of the left ventricle (LV) and reduced LV fractional shortening. Apoptosis and LC3-II expression in cardiac tissue were increased by imatinib. Co-treatment with 3MA and imatinib further impaired imatinib-induced cardiac apoptosis and LV dysfunction. This study suggests that imatinib induces cardiomyocyte apoptosis, leading to cardiac dysfunction. Imatinib increases cardiomyocyte autophagy as a consequence of apoptosis and autophagy has a pro-survival role in imatinib-induced cardiac impairment.

1. Introduction

Cancer is an age-related disease and leading cause of death in developed countries [1]. In aging societies, the number of cancer patients is increasing and recent anti-cancer therapy using chemotherapeutic agents has markedly improved the prognosis of cancer patients, resulting in a larger population of long-term cancer survivors [2]. However, chemotherapy-induced cardiotoxicity remains a significant adverse effect and is of considerable interest [3]. Among chemotherapy-induced cardiotoxicities, those of doxorubicin are well-known and have been investigated [4–6]. Recently, cardiac complications of targeted chemotherapeutic agents, such as tyrosine-kinase inhibitors, were reported [7–9].

Imatinib is a small-molecule inhibitor of tyrosine kinase, and has markedly improved the clinical outcomes of chronic myelogenous leukemia (CML) and gastrointestinal stromal tumors (GIST) [10,11]. In CML and GIST, a specific Bcr-Abl fusion protein and c-kit are respectively observed, and are both inhibited by imatinib [12,13]. In addition to these two proteins, imatinib inhibits c-Abl and platelet-derived growth factor receptors (PDGFRs) [7,14]. Cardiac disorders by imatinib have received considerable attention as important adverse effects because severe cardiac failure has also been reported [7]. Although the rate of congestive heart failure varies [15–17], elderly patients with previous cardiac disorder were reported to be susceptible to imatinib-induced heart failure and cardiac complications remain important adverse effects of imatinib-based therapy [18,19]. In animal *in vivo* and *in vitro* studies, imatinib also induced cardiotoxicity, and several mechanisms of imatinib-induced cardiotoxicity have been proposed, including endoplasmic reticulum (ER) stress, mitochondrial damage [7,10,20], and impairment of cardiac progenitor cells [9].

* Corresponding author at: Department of Clinical Pharmacology, Division of Pathological Science, Kyoto Pharmaceutical University, 5 Misasagi Nakauchi-cho, Yamashina-ku, Kyoto, 607-8414, Japan.
E-mail address: kobara@mb.kyoto-phu.ac.jp (M. Kobara).

https://doi.org/10.1016/j.toxrep.2021.05.008
Received 31 December 2020; Received in revised form 9 May 2021; Accepted 17 May 2021
Available online 19 May 2021

Autophagy was demonstrated to be a self-proteolysis system characterized by the sequestration and enclosure of intracellular components, and their following degradation by lysosomes [21,22]. This phenomenon is conserved in many species from yeast to mammals and is known as a cell survival mechanism during malnutrition [22]. In this autophagic process, initiation stimuli, such as AMP activated kinase (AMPK) activation, precedes the complex formation of beclin 1 and vesicle-mediated vacuolar protein sorting 34, which promotes the cascade of phagophore formation [23]. After elongation of the phagophore by autophagy-related gene (Atg) proteins, microtubule-associated protein light chain 3B (LC3-II) associates with the double membrane of the autophagosome. Autophagosomes are tagged by ubiquitination and fuse with lysosomes to form autolysosomes, and mature acidic autolysosomes are then degraded by lysosomal enzymes [23,24]. Autophagy also mediates development and differentiation, and the impairment of autophagy was reported to lead to abnormal growth and diseases, including muscular disorders and neural degradation [25]. On the other hand, autophagy-related cell death has been reported under specific pathological conditions [26–32].

In cardiac tissue, autophagy mediates development and function, and is also observed in failing myocardium in human and animal models [26,33–35] such as dilated cardiomyopathy [33], ischemic heart diseases [34], and pressure overload-induced cardiomyopathy [35]. In ischemic heart diseases, autophagy induction by food restriction improved cardiac function [36]. On the other hand, in terminal heart failure, autophagic myocyte death was found [37]. Myocyte loss due to fatal injury, such as necrosis, apoptosis, and autophagy, leads to cardiac dysfunction and exacerbates cardiac failure because cardiomyocytes are terminally differentiated cells and lose their proliferative ability [26,38]. The role of autophagy, which is pro-survival or pro-death, in these failing conditions is not fully understood. Recently, imatinib was reported to induce autophagy in neuroblastoma cells [39]. Therefore, the purpose of this study was to assess whether imatinib induces cardiac failure and autophagy, and its roles in cardiomyocyte death and heart function using cultured neonatal cardiomyocytes and the adult heart.

2. Methods

All procedures complied with the ARRIVE guidelines and conformed to the *Guide for the Care and Use of Laboratory Animals* published by the US National Institutes of Health. The protocol was approved by the Animal Care and Use Committee of Kyoto Pharmaceutical University.

2.1. In vitro culture of neonatal cardiomyocytes

Neonatal rat ventricular myocytes were isolated from Wistar rats (Japan SLC Inc., Hamamatsu, Japan) and cultured in Dulbecco's Modified Eagle's Medium (DMEM) as described previously [40]. Briefly, the left ventricle was minced by scissors and digested using 0.2 % collagenase at 37 °C. After aggregated tissue was removed by filtration, cells were then pre-plated for 1.5 h to remove non-myocytes. Nonadherent cardiomyocytes were plated at 2×10^5 cells/24-well glass-base plate for microscopic analyses or 2.5×10^6 cells/6-cm dish for other analyses in DMEM containing 10 % fetal bovine serum (FBS), gentamycin, and bromodeoxyuridine (BrdU 10^{-4} mol/L) for 2 days. BrdU was used to prevent the proliferation of contaminated nonmyocytes. The cardiomyocytes were then incubated in DMEM containing 5 % FBS without BrdU and gentamycin. All experiments were performed 48−72 h after this incubation.

2.1.1. Experimental protocols for cultured cardiomyocytes

Cultured cardiomyocytes were washed with phosphate-buffered saline (PBS), followed by a final incubation in serum-deprived DMEM. During the final incubation, cardiomyocytes were incubated with imatinib (1–10 μmol/L) for 6 h. To evaluate the roles of autophagy in imatinib-induced myocyte injury, pharmacological inhibition by 3-methyl-adenine (3MA) was performed in addition to imatinib administration. To examine the source of reactive oxygen species (ROS) production by imatinib, myocytes were stimulated by 10 μmol/L of imatinib in the presence of butylated hydroxyanisol (BHA) (10 μmol/L), a mitochondrial ROS scavenger.

2.1.2. Western blot analysis

Cardiomyocytes were lysed in RIPA lysis buffer (Santa Cruz, CA, USA) containing 1 % Protease Inhibitor Cocktail (Nacalai Tesque, Inc., Kyoto, Japan) at 4 °C for 10 min. Cell extracts were centrifuged at 3000×*g* at 4℃ for 10 min and supernatants were used as protein extracts. Protein concentrations in protein extracts were assessed by the Lowry methods. Equal amounts of protein extracts were then subjected to polyacrylamide gel electrophoresis, followed by electroblotting onto polyvinylidene difluoride membranes. After blocking with 5 % skim milk in PBS for 3 h, the membranes were incubated with rabbit polyclonal antibody against microtubule-associated protein 1 light chain 3 protein (LC3, 1:1000, M115-3, MBL Co. Ltd., Ina, Japan), mouse monoclonal antibody against beclin 1 (1:1000, 612112, BD Biosciences, NY, USA), or goat polyclonal antibody against cathepsin D (1:1000, sc-6487, Santa Cruz, CA, USA) at 4℃ overnight. Then, the membranes were incubated with horseradish peroxidase (HRP)-conjugated anti-rabbit IgG (1:1,000, GE Healthcare, UK, for LC3), HRP-conjugated anti-mouse IgG (1:1,000, GE Healthcare, UK, for beclin 1), or HRP-conjugated anti-goat IgG (1:1,000, sc-2354, Santa Cruz, CA, USA, for cathepsin D) as secondary antibodies at room temperature for 2 h and processed for chemiluminescent detection using enhanced chemiluminescence (ECL, GE healthcare, UK). Actin (1:2,000, mouse anti-actin monoclonal antibody, Chemicon International, Temecula, USA; 1:2,000, anti-mouse IgG HRP conjugated, GE Healthcare, UK) was used as a loading control. The protein amounts of LC3-II (16 kD), beclin 1 (61 kD), mature cathepsin D (33 kD), and actin (43 kD) on Western blotting were quantified by densitometry.

2.1.3. Flow cytometric analysis of mature autolysosomes

Mature autolysosomes were assessed by acridine orange staining to detect acidic vesicular organelles in the cytoplasm. At the end of the experimental period, myocytes were incubated with acridine orange (2.5 μg/mL) for 15 min. After washing with PBS, myocytes were detached from the culture dish using trypsin and collected. After centrifugation and washing with PBS, cardiomyocytes were suspended in FACS buffer containing PBS, 0.5 % bovine serum albumin (BSA), and 0.5 mol/L ethylenediaminetetraacetic acid (EDTA) (1.5×10^6 cells/mL), and counted by flow cytometry (FACS Caliber flow cytometer, Becton-Dickinson, Franklin Lakes, NJ, USA). Green and red fluorescence in 10×10^4 cells were analyzed using the FL1 and FL3 channels, respectively. CellQuest software was used to assess acridine orange-positive cardiomyocytes.

2.1.4. Intracellular ROS

Intracellular ROS production in cultured cardiomyocytes was evaluated using a fluorescent probe, dihydroethidium (DHE). DHE (2.5 μmol/L) was added to the cardiomyocytes 30 min before the end of the experiment. After washing with PBS, DHE fluorescence was examined using the optical microscope system (Olympus IX71, Olympus Japan, Tokyo, Japan). Fluorescence emission at 575 nm was acquired with excitation at 540 nm. The average fluorescence intensity in myocytes was quantified using ScnImage software.

2.1.5. Mitochondrial ROS

A fluorescent probe, MitoSOX (Molecular Probes, Eugene, USA), was used to evaluate mitochondrial ROS production in cultured cardiomyocytes. MitoSOX (0.5 μmol/L) was added to the cardiomyocytes 15 min before the end of the experiment. After washing with PBS, confocal fluorescence images were obtained using the fluorescence microscope LSM510 (Carl Zaiss Co., Oberkochen, Germany). Fluorescence

emission at 590 nm was acquired with excitation at 514 nm. The average fluorescence intensity in myocytes was quantified using ScnImage software.

2.1.6. Mitochondrial membrane potential

Mitochondrial transmembrane potential was assessed using the fluorescent probe JC-1 (Molecular Probes, Eugene, USA). Cardiomyocytes were incubated with JC-1 (10 μmol/L) at 37 °C for 5 min before the end of the experimental period. After washing with PBS, confocal fluorescence images were obtained using the fluorescence microscope LSM510 (Carl Zaiss, Oberkochen, Germany). Fluorescence emission at 527 and 590 nm was measured after excitation at 488 nm. The ratio of red fluorescence area to the total mitochondrial area was quantified using ScnImage software.

2.1.7. Assessment of myocyte apoptosis

Cultured cardiomyocytes were fixed with 2 % phosphate buffered paraformaldehyde for 5 min followed by 5-minute permeabilization with 0.5 % Triton X-100. Nuclei were then stained with 4′,6′-diamidino-2 phenylindole (DAPI). Fragmented or condensed nuclei were identified as apoptotic nuclei. Using ten photomicrographs of randomized and non-overlapping fields, the number of apoptotic nuclei was counted and the degree of apoptosis was expressed as a percentage of the total number of nuclei counted.

2.1.8. Caspase-3 activity

Caspase-3 activity was assessed using an APOCYTO Caspase-3 Colorimetric Assay Kit (MBL Co. Ltd., Nagoya, Japan). According to the manufacturer's instructions, cultured cardiomyocytes were collected by scraping and centrifuged at 400×g at 4 °C for 5 min. Then, cardiomyocytes were lysed in lysis buffer (in kit) and clarified by centrifugation at 10,000×g at 4 °C for 5 min. Supernatants of cell extracts were then incubated with 10 mmol/L of DTT and the labeled caspase-3 substrate DEVD- *p*-nitroanilide (DEVD-pNA) at 37 °C for 24 h (in kit). Caspase-3 activity was quantified by the production of substrate cleavage (pNA) at 405 nm. Protein concentrations of cell lysates were measured by the Bradford method.

2.2. In vivo experiments

2.2.1. Animals and experimental protocol

Male C57BL/6 mice (20–25 g) were purchased from Japan SLC Inc. (Hamamatsu, Japan) and divided into five groups: 1) control group (cont), 2) low-dose imatinib-treated (50 mg/kg/day) group (imatinib-50), 3) high-dose imatinib-treated (200 mg/kg/day) group (imatinib-200), 4) co-treatment with 3MA and high-dose imatinib group (3MA + imatinib-200), and 5) 3MA-treated group (3MA). Imatinib was orally administered by gavage every day for 5 weeks in low- and high-dose imatinib-treated groups, and a similar volume of tap water was administered by gavage as a placebo in control and 3MA groups. 3MA (50 mg/kg) was administered by intraperitoneal injection weekly throughout the experimental period. After 5 weeks, mice were subjected to echocardiography under light anesthesia. Then, the mice were sacrificed, and the heart and lung were excised and weighed. The left ventricle (LV) was separated from the right ventricle and cut transversely at the middle level. The apical part of the LV was frozen for Western blotting and the basal part was fixed for histological examination.

2.2.2. LV echocardiographic studies

Transthoracic echocardiography was performed to evaluate the cardiac function using a 15-MHz sector scan probe (SONOS 5500, Phillips Medical Systems Japan, Tokyo, Japan) at the end of the experimental period. The LV end-diastolic diameter (LVEDd) and end-systolic diameter (LVEDs) were measured at the level of the papillary muscle using M-mode recordings. LV fractional shortening (FS) was calculated as FS (%) = ((LVEDd-LVEDs)/LVEDd) ×100.

2.2.3. Histological analysis

After fixation with 4 % paraformaldehyde phosphate buffer, pH 7.4, LV tissue was embedded in paraffin. Tissue samples were cut into 4-μm sections and stained with Masson's trichrome or Sirius Red. Cardiomyocyte size was quantitatively evaluated using the cross-sectional area of myocytes in Masson's trichrome-stained sections. Twenty independent fields of the myocardium from each mouse were photographed using an optical microscope system (Olympus IX71, Olympus Japan, Tokyo, Japan). The circumferences of 200 myocytes in true transverse sections, defined as those with circular capillary profiles and myofiber shapes, were traced and inner pixels were counted. Interstitial fibrosis was analyzed using Sirius Red-stained sections and five independent fields of the myocardium from each mouse were photographed. Intramuscular pink-red pixels were counted as the area of interstitial fibrosis, and the ratio was calculated as the sum of the interstitial fibrosis area divided by the sum of all tissue areas in the field.

2.2.4. In situ detection of apoptosis

Apoptotic cell death was evaluated by the TUNEL method using an APOP TAQ kit (Oncor, Gaithersburg, MD). LV sections (4-μm-thick) were deparaffinized and incubated with proteinase K (20 μg/mL) at room temperature for 15 min. To block internal peroxidase activity, samples were treated with 3 % hydrogen peroxidase for 5 min. After applying equilibrium buffer (in kit), the specimens were incubated with terminal deoxynucleotidyl transferase at 37 °C for 1 h. The reaction was finalized by adding stop solution (in kit). Specimens were then incubated with antidigoxigenin peroxidase solution at room temperature for 30 min and peroxidase activity was visualized using 0.025 % 3,3′-diamino benzidine solution. The sections were counterstained with hematoxylin to visualize the nuclei. We counted 3000 nuclei using a light microscope and calculated the ratio of TUNEL-positive nuclei.

2.2.5. Western blot analysis

LV tissues were minced and homogenized in Tris buffer containing 50 mmol/L of Tris-HCl, 1 mmol/L of EDTA·2Na, 1 mmol/L of EGTA, 1 % Triton X100, and 1 % Protein Inhibitor Cocktail (Nacalai Tesque Inc. Kyoto, Japan), pH 7.4. Homogenates were then centrifuged at 8000×*g* at 4 °C for 10 min. Supernatants were used for protein extraction. The protein concentrations of extracts were measured using the Lowry method. After electrophoresis and electroblotting onto PVDF membranes, the membranes were incubated with rabbit polyclonal antibody against LC3 (1:1000, M115-3, MBL Co. Ltd., Ina, Japan) followed by incubation with HRP-conjugated anti-rabbit IgG (1:1,000, GE Healthcare, UK) (mentioned above in Methods *in vitro* experiments). Actin was used as a loading control. The protein amounts of LC3-II and actin on Western blotting were quantified by densitometry.

2.2.6. Statistical analysis

All values are expressed as the mean ± SEM. Statistical analysis was performed by one-way ANOVA combined with Fisher's multiple comparison test (Figs. 1a, 2 b, 3 d, 5 a–c, 6 a, b, 7 c, d, 8 b, and Table 1) or the Student's *t*-test (Figs. 1b, c, 3 g, and 4 c, f). Values of $p < 0.05$ were considered significant.

3. Results

3.1. In vitro experiments

3.1.1. Imatinib induced autophagy in cardiomyocytes

Imatinib increased the expression of the autophagosome indicator LC3-II in a dose-dependent manner and imatinib (10 μmol/L) significantly increased the level of LC3-II expression by 2.5-fold (Fig. 1a). Imatinib (10 μmol/L) also significantly increased beclin 1, another indicator of autophagosomes, and mature cathepsin D expression, an

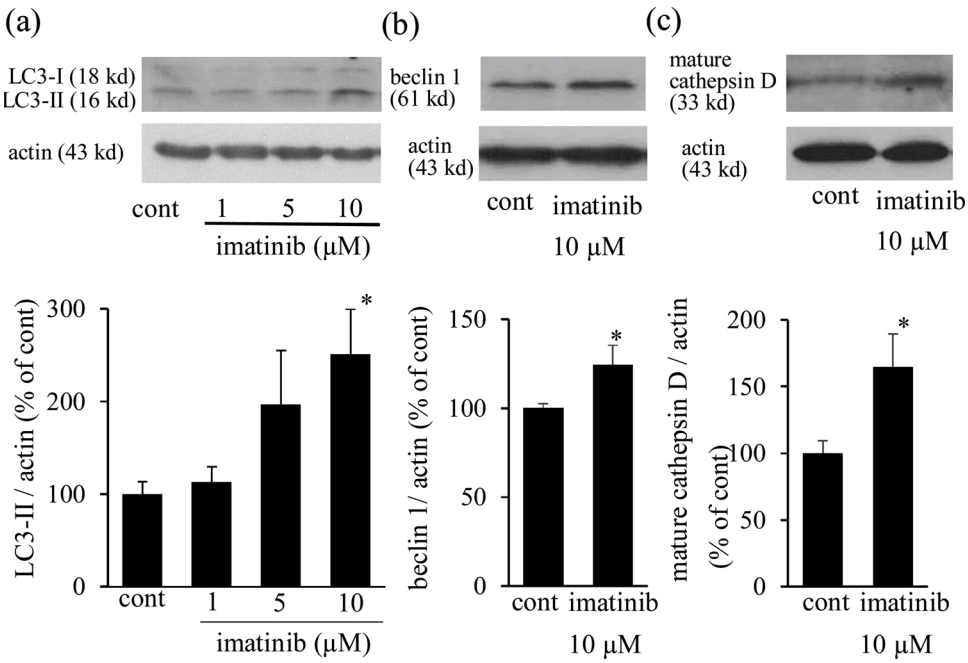

Fig. 1. Imatinib increases LC3-II, beclin 1, and mature cathepsin D expression. Neonatal cultured cardiomyocytes were treated with imatinib (1-10 μmol/L) for 6 h. Representative expression of LC3-I and LC3-II (a, top panel), beclin 1 (b, top panel), and mature cathepsin D (c, top panel). Actin was used as a loading control. The expression levels of LC3-II (a, bottom panel), beclin 1 (b, bottom panel), and mature cathepsin D (c, bottom panel) were quantified and presented as bar graphs (n = 6-8). * $p < 0.05$ *versus* cont. LC3: microtubule-associated protein 1 light chain 3 protein.

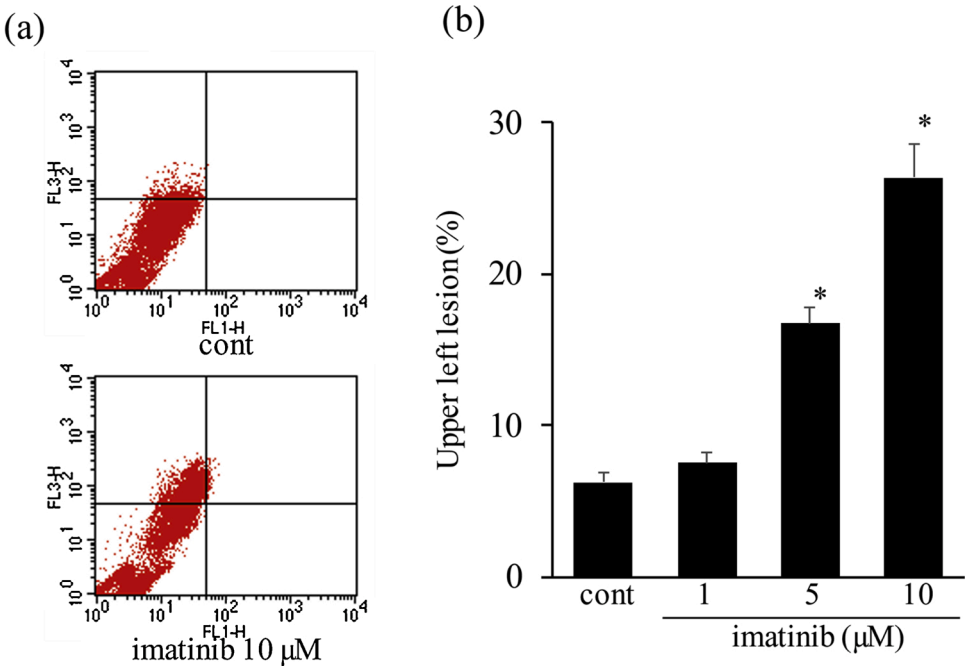

Fig. 2. Imatinib increases acridine orange-stained mature autolysosome expression in cultured cardiomyocytes. (a) Representative plots of acridine orange-stained myocytes. Neonatal cultured cardiomyocytes were treated with imatinib (1-10 μmol/L) for 6 h. After staining with acridine orange, myocytes were analyzed by flow cytometry. (b) Quantitative analysis of acridine orange-stained organelles. Bars indicate the average percentage of myocytes with high red-low green relative staining (upper left column) (n = 5-6). * $p < 0.05$ *vs.* cont.

indicator of lysosomal function (Fig. 1b, c). In addition, imatinib increased acridine orange-stained mature autolysosome expression in a dose-dependent manner, and a significant increase was noted after imatinib treatment at 5 and 10 μmol/L (Fig. 2a, b). Imatinib induced autophagy in a dose-dependent manner and 10 μmol/L of imatinib was used in the following examinations.

3.1.2. *Imatinib increased the mitochondrial ROS level and impaired mitochondrial membrane potential in cardiomyocytes*

Imatinib treatment (10 μmol/L) increased the intracellular ROS level detected by DHE staining (Fig. 3a, b). The imatinib-induced DHE fluorescence was markedly reduced by co-treatment with BHA, a mitochondrial ROS scavenger (Fig. 3c, d), suggesting that imatinib increased ROS production *via* mitochondria. We also confirmed mitochondrial ROS generation by imatinib using the mitochondrial ROS indicator MitoSOX. Imatinib treatment (10 μmol/L) increased mitochondrial ROS (Fig. 3e–g). ROS-producing damaged mitochondria elicit the loss of mitochondrial membrane potential. JC-1 staining revealed that imatinib reduced red fluorescence and increased green fluorescence in mitochondria, reflecting the loss of mitochondrial membrane potential (Fig. 4a–c).

3.1.3. *Imatinib induced apoptosis in cardiomyocytes*

Imatinib treatment (10 μmol/L) significantly increased condensed and fragmented nuclei, detected by nuclear staining with DAPI, suggesting that imatinib increased apoptotic nuclei (Fig. 4d–f). The ratio of

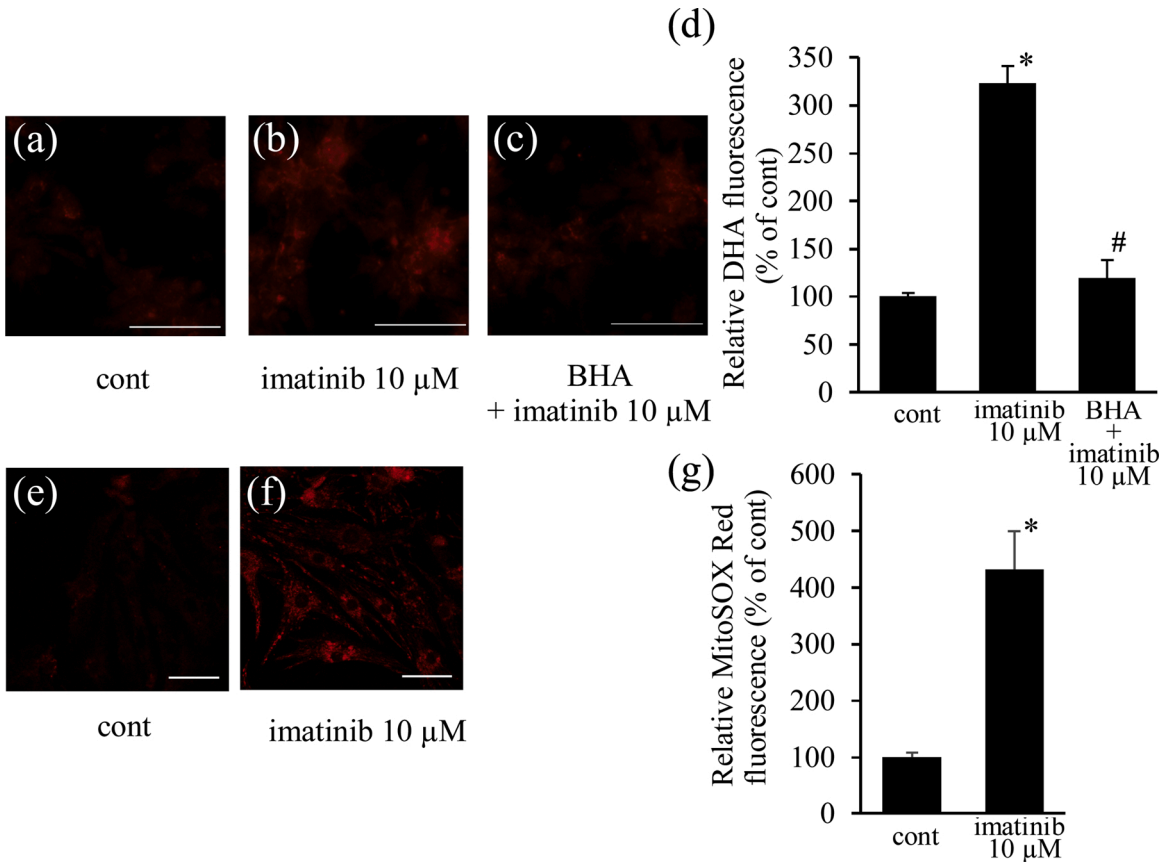

Fig. 3. Imatinib induces mitochondrial ROS production. Neonatal cultured cardiomyocytes were treated with imatinib (10 μmol/L) for 6 h in the presence or absence of butylated hydroxyanisol (BHA) (10 μmol/L), a mitochondrial ROS scavenger, and stained with DHE, an intracellular ROS indicator (a - c). Imatinib increased the intensity of DHE fluorescence and co-incubation with BHA attenuated it (d). Cultured cardiomyocytes were next stained with MitoSOX, a mitochondrial ROS indicator (e, f). Imatinib increased the intensity of MitoSOX fluorescence (g). Intensities of fluorescence were analyzed and shown as relative fluorescence intensities to cont (d, g) (n = 7). Bars indicate 100 μm (a – c), 50 μm (e, f). * $p < 0.05$ *vs.* cont, # $p < 0.05$ *versus* imatinib.

apoptotic nuclei was increased 4-fold by imatinib (10 μmol/L), consistent with the synchronous increase in caspase-3 activity in cardiomyocytes (Fig. 5a, b). Therefore, imatinib increased apoptosis in cardiomyocytes.

3.1.4. Role of autophagy in imatinib-induced apoptosis in cardiomyocytes

We next examined the effects of autophagy inhibition on myocyte apoptosis. First, we confirmed that 3MA significantly inhibited imatinib-induced autophagy using acridine orange staining (Fig. 5c). Autophagy inhibition by 3MA further increased the ratio of apoptotic nuclei and caspase-3 activity compared with imatinib-treated myocytes (Fig. 5a, b).

3.2. In vivo experiments

3.2.1. Imatinib increased LC3-II expression in cardiac tissue

The expression of LC3-II protein in cardiac tissue is shown in Fig. 5a and b. LC3-II protein expression was increased by imatinib in a dose-dependent manner and imatinib (200 mg/kg) significantly increased the expression level of LC3-II, suggesting that it induced autophagy in cardiac tissue (Fig. 6a). In addition, 3MA reduced this imatinib-induced LC3-II expression (Fig. 6b).

3.2.2. Effects of imatinib on body and organ weights, and the role of imatinib-induced autophagy

Body and organ weights of mice at the end of the experimental period are shown in Table 1. Significant differences were not observed in body weight among all groups. Ratios of heart weight/body weight, LV weight/body weight, and lung weight/body weight were increased by imatinib treatment in a dose-dependent manner, and imatinib (200 mg/kg) significantly increased these ratios. Co-administration of 3MA and imatinib (200 mg/kg) further increased these ratios.

3.2.3. Cardiac function in mice treated with imatinib and the role of imatinib-induced autophagy

At the end of the experimental period cardiac function was examined by echocardiography (Table 1). Imatinib dilated LV and reduced LV systolic function in a dose-dependent manner, and significant differences were observed at 200 mg/kg. In addition, 3MA further impaired LV dilatation and augmented the reduction in left ventricular fractional shortening.

3.2.4. Cardiac histomorphometry after imatinib treatment and the role of imatinib-induced autophagy

We examined the effects of imatinib on cardiomyocyte size and interstitial fibrosis in cardiac tissue, and evaluated the role of autophagy in these histological changes. Representative photomicrographs of Masson's trichrome- and Sirius Red-stained LV sections at the end of the experiment are shown in Fig. 7a and b, respectively. Myocyte size was slightly but significantly increased by imatinib (200 mg/kg), and co-administration with 3MA further increased it (Fig. 7c). The ratio of interstitial fibrosis was not affected in the imatinib (200 mg/kg)-treated group. However, co-administration with 3MA markedly increased the fibrosis area (Fig. 7d). Therefore, cardiac autophagy alleviated myocyte hypertrophy and interstitial fibrosis during imatinib treatment.

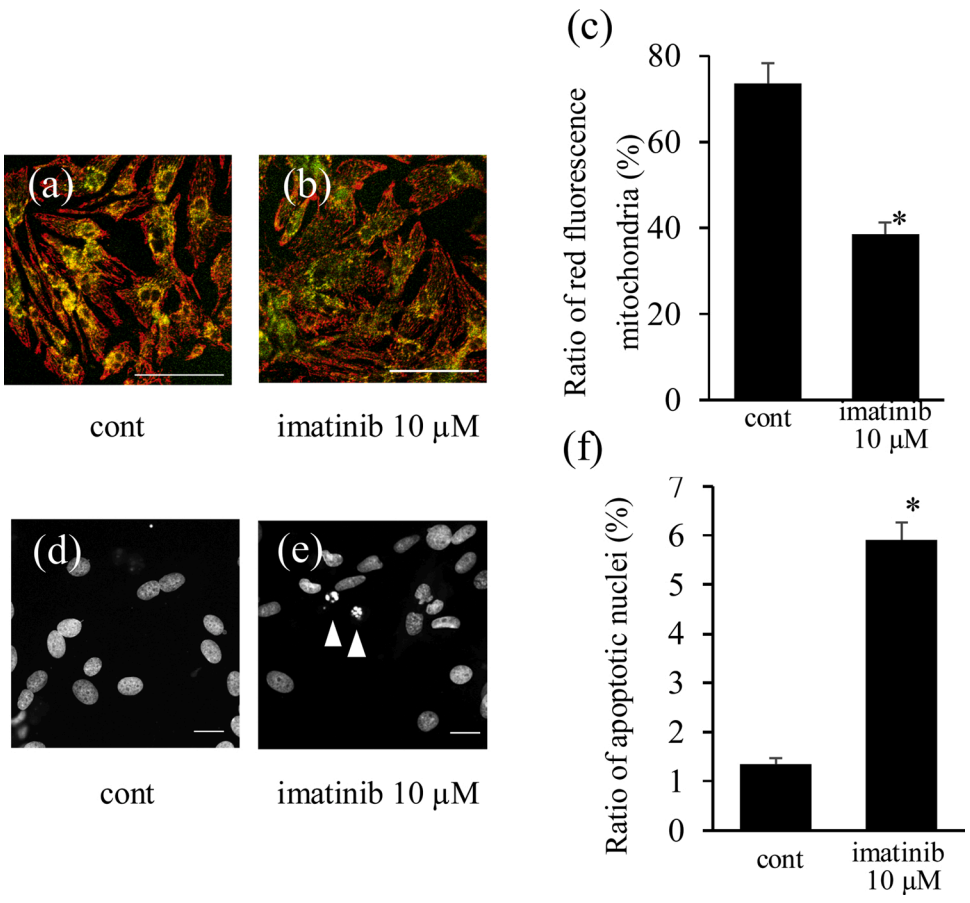

Fig. 4. Imatinib reduces the mitochondrial membrane potential accompanied by myocyte apoptosis. Neonatal cultured cardiomyocytes were treated with imatinib (10 μmol/L) for 6 h and stained with JC-1, an indicator of mitochondrial membrane potential (a, b). Imatinib reduced the red fluorescence in mitochondria and increased the green fluorescence in mitochondria (dissipated mitochondrial membrane potential). The ratio of red fluorescence in mitochondria was analyzed (c) (n = 7). The morphology of nuclei was assessed by nuclear staining with DAPI (d, e). Arrowheads indicate apoptotic nuclei (e). Ratio of apoptotic cardiomyocytes after imatinib treatment (f) (n = 9). Bars indicate 100 μm (a, b) and 20 μm (d, e). * $p < 0.05$ *versus* cont.

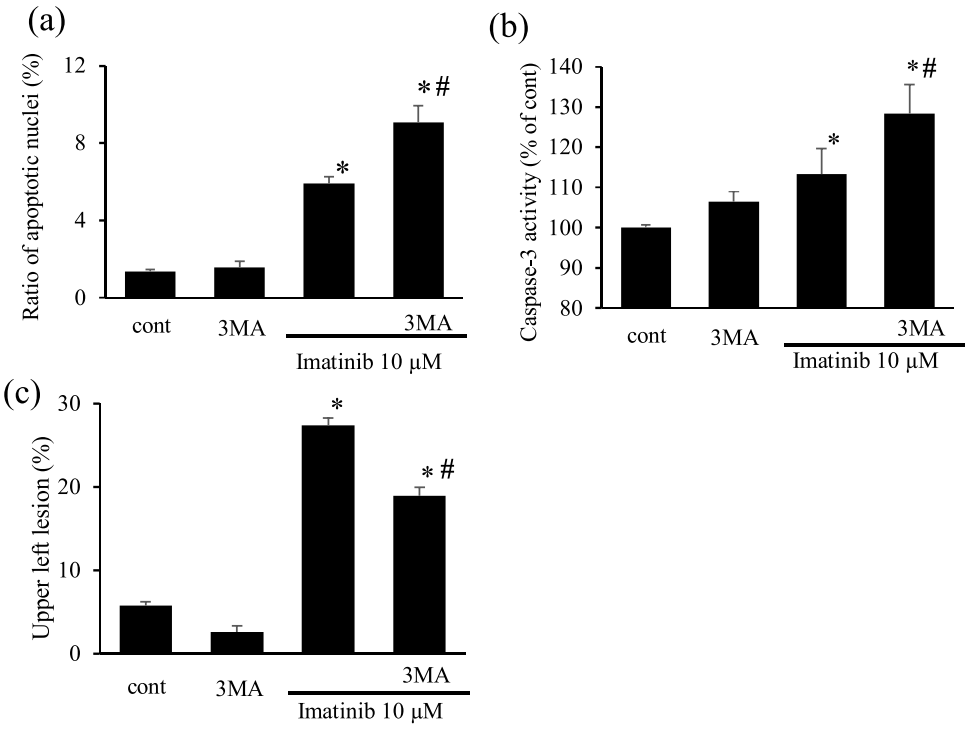

Fig. 5. Imatinib induces apoptosis and autophagy inhibition by 3MA further exacerbated it in cardiomyocytes (a, b). Percentage of apoptotic cardiomyocytes after imatinib treatment (10 μmol/L for 6 h) in the presence or absence of 3MA (a) (n = 9). Caspase-3 activity in myocytes after treatment with imatinib in the presence or absence of 3MA (b). Results were expressed as the relative differences to the control group (cont) (n = 5-8). Effects of 3MA, an autophagy inhibitor, on imatinib-induced acridine orange-stained autolysosome expression in cultured cardiomyocytes (c). The bar graph indicates the average percentage of myocytes with high red-low green relative staining (c) (n = 6-7). * $p < 0.05$ *versus* cont, # $p < 0.05$ *versus* imatinib.

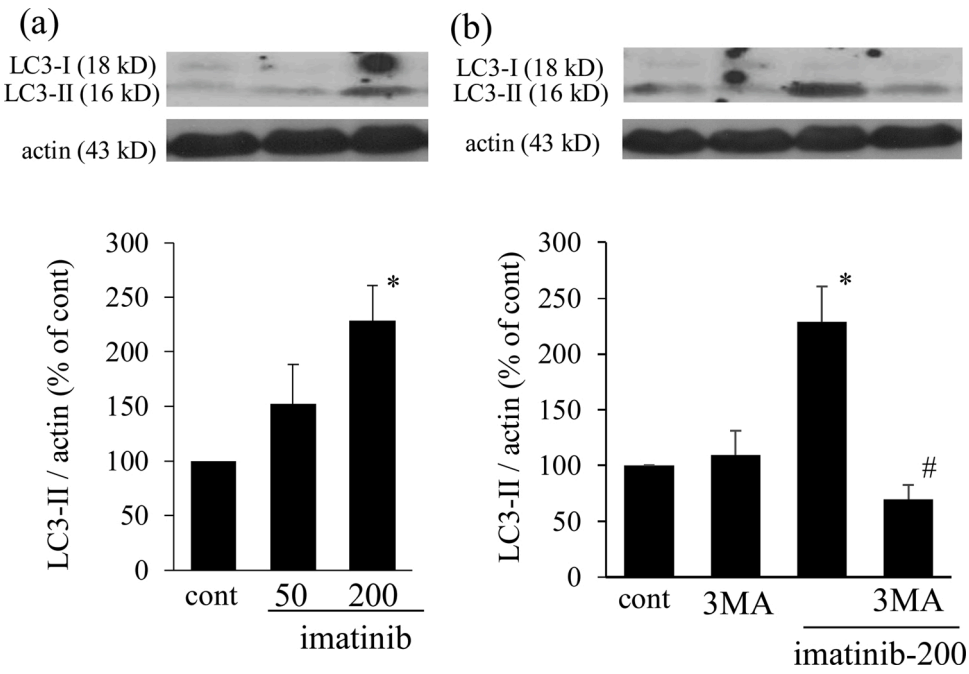

Fig. 6. Imatinib increases LC3-II expression in cardiac tissue. Mice were treated with imatinib (50 or 200 mg/kg/day) for 5 weeks. Western blots of LC3-I and LC3-II (a, top panel), and expression levels of LC3-II (a, bottom panel) in cardiac tissue after imatinib treatment (n = 5). Effects of 3MA (50 mg/kg/week, i.p.) on imatinib-induced LC3-II expression (b) (n = 5). * $p < 0.05$ *versus* cont, # $p < 0.05$ *versus* imatinib-200.

Table 1
Body and organ weights, and echocardiographic assessment at the end of the experiment. (n = 5–8).

	cont	imatinib-50	imatinib-200	3MA+imatinib-200	3MA
BW (g)	25.8 ± 0.8	25.5 ± 1.1	23.9 ± 0.5	24.0 ± 0.5	26.3 ± 0.9
HW/BW (mg/g)	4.50 ± 0.11	4.65 ± 0.09	4.83 ± 0.12*	5.19 ± 0.09*,#	4.47 ± 0.16
LVW/BW (mg/g)	3.08 ± 0.06	3.30 ± 0.11	3.52 ± 0.09*	3.90 ± 0.09*,#	3.16 ± 0.10
LungW/BW (mg/g)	4.75 ± 0.11	5.03 ± 0.06	5.18 ± 0.04*	5.68 ± 0.13*,#	4.63 ± 0.25
LVDd (mm)	2.62 ± 0.07	2.66 ± 0.15	3.09 ± 0.06*	3.47 ± 0.08*,#	2.74 ± 0.07
LVFS (%)	63.0 ± 2.0	62.7 ± 3.6	50.5 ± 0.8*	40.4 ± 2.6*,#	58.0 ± 1.3

BW: body weight, HW: heart weight, LVW: left ventricular weight, LungW: lung weight, LVDd: left ventricular end-diastolic dimeter, LVFS: left ventricular fractional shortening.
* $p < 0.05$ *versus* cont.
# $p < 0.05$ *versus* imatinib-200.

3.2.5. Apoptosis in cardiac tissue after imatinib treatment and the role of imatinib-induced autophagy

In situ detection of apoptosis in cardiac tissue was performed by TUNEL staining (Fig. 8a, b). Representative photomicrographs of LV sections after imatinib treatment are shown in Fig. 8a. The ratio of TUNEL-positive nuclei slightly but significantly increased in the imatinib (200 mg/kg)-treated group (Fig. 8b). In addition, this ratio was further increased by co-administration with 3MA.

4. Discussion

The present study demonstrated that imatinib increases cardiomyocyte autophagy and apoptosis in association with mitochondrial ROS production and loss of mitochondrial membrane potential in neonatal cultured cardiomyocytes. The inhibition of myocyte autophagy exacerbated myocyte apoptosis. In addition, in *in vivo* experiments, imatinib increased cardiac apoptosis and autophagy in association with cardiac dysfunction, and an autophagy inhibitor further increased apoptosis, and exacerbated left ventricular dysfunction and histological impairment.

In the present study, we examined the dose-dependent effects of imatinib from 1 to 10 μmol/L on cultured neonatal cardiomyocytes and 50 to 200 mg/kg/day on adult mice. In the clinical treatment of CML and GIST, imatinib is administered daily at 400–800 mg, and the maximum concentration was reported to be almost 5–10 μmol/L at 28 days of continuous drug treatment. Therefore, we examined imatinib at 1–10 μmol/L in this experiment. In previous *in vitro* studies of cultured neonatal cardiomyocytes and myoblast cell lines, such as H9C2 and HL1, different doses of imatinib from 0.1 to 100 μmol/L were examined [7,16,20,41]. In these reports, fatal cell injury and mitochondrial damage were observed at 5 μmol/L or higher [7,41]. The present study demonstrated that imatinib (10 μmol/L) increases mitochondrial ROS in association with disruption of mitochondrial membrane potential, leading to myocyte apoptosis, consistent with previous studies. In addition, in the *in vivo* study, we administered imatinib at 50 and 200 mg/kg/day, which is higher than the human clinical dose (8–15 mg/kg/day). As imatinib is metabolized faster in mice than in humans [42], oral administration of imatinib at 200–400 mg/kg/day was reported to be comparably effective [7,43]. In the previous animal report, mice treated with imatinib (50 mg/kg/day) did not exhibit overt cardiac damage based on the ratio of heart to body weights, and only had reduced kinase phosphorylation of Akt and extracellular signal-regulated kinase (ERK) [16]. In the present examination, imatinib (50 mg/kg/day) did not alter the ratio of heart weight to body weight (Table 1), consistent with previous reports

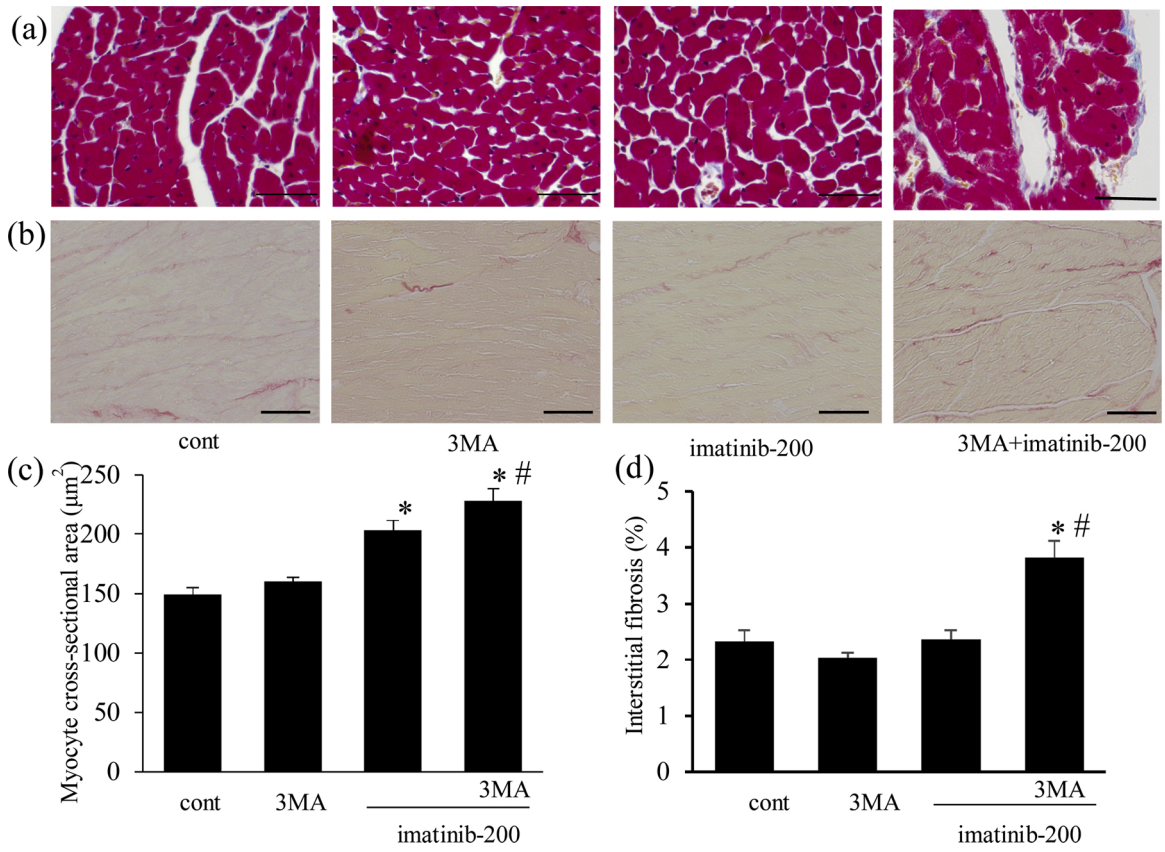

Fig. 7. Effects of imatinib, and the roles of autophagy in its effects on myocyte hypertrophy and interstitial fibrosis. Imatinib induced myocyte hypertrophy but not interstitial fibrosis in cardiac tissue, whereas autophagy inhibition exacerbated both histological changes. Mice were treated with imatinib (200 mg/kg/day) with or without 3MA (50 mg/kg/week, i.p.) for 5 weeks. Light micrographs show Masson's trichrome-stained (a) and Sirius Red-stained LV cross-sections (b) at the end of the experiment. Bars indicate 50 μm (a) or 100 μm (b). (c) Cardiomyocyte cross-sectional area in LV (n = 8). (d) Percentage of interstitial fibrosis in LV (n = 8). * $p < 0.05$ *versus* cont. # $p < 0.05$ *versus* imatinib-200.

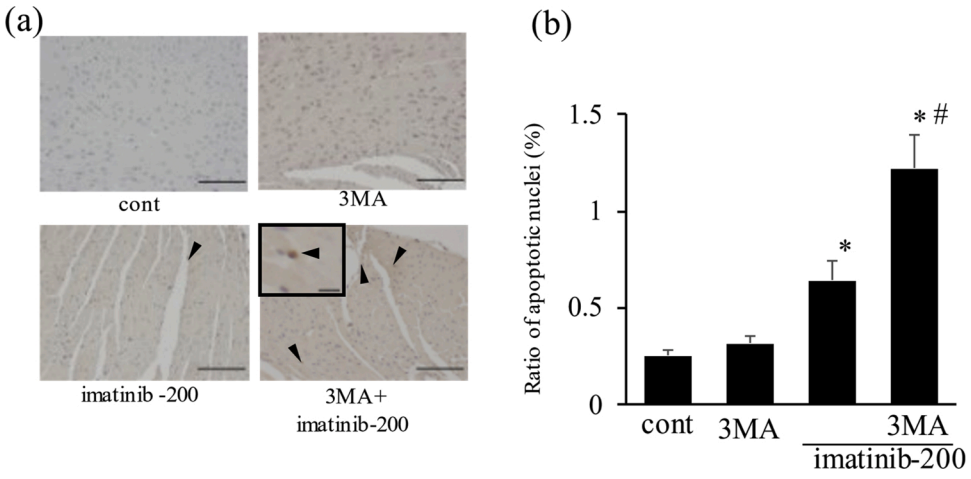

Fig. 8. Imatinib induced apoptosis in cardiac tissue, which was further increased by autophagy inhibition. Light micrographs show terminal deoxynucleotidyl transferase-mediated dUTP nick end-labeling (TUNEL) staining of cardiac tissues at the end of the experiment (a). Arrowheads indicate apoptotic nuclei. Scale bars, 100 μm. *inset*: the TUNEL-positive nucleus under high magnification. Scale bars, 10 μm. Ratio of TUNEL-positive nuclei after imatinib treatment (b) (n = 8). * $p < 0.05$ *versus* cont, # $p < 0.05$ *versus* imatinib-200.

[16]. Therefore, in the present study, the effects of imatinib at 200 mg/kg/day on cardiotoxicity in the mice model were mainly examined and our findings of cardiotoxicity were due to the clinical dose of imatinib.

In the present study, imatinib increased myocyte ROS, which were diminished by BHA, a mitochondrial ROS scavenger, and it also increased the fluorescence of the mitochondrial ROS indicator MitoSOX, suggesting that imatinib increased mitochondrial ROS production. Under physiological conditions, mitochondria generate ROS through oxidative phosphorylation and these ROS are promptly removed by Mn SOD. However, under pathological conditions, excessive mitochondrial ROS injure mitochondria and reduce their membrane potential [44,45]. In the present study, imatinib depleted the mitochondrial membrane potential in association with ROS production, consistent with prior studies [7,46]. Injured mitochondria are a major inducer of myocyte apoptosis due to the following cytochrome c release and caspase 3 activation [26,38]; therefore, the increased apoptotic nuclear fragmentation and caspase-3 activation by imatinib observed in the present

study may have been due to mitochondrial injury. On the other hand, an increase in mitochondrial ROS production by mitochondrial electron transport chain inhibition induces autophagy [30], and oxidized and damaged mitochondria are expected to induce autophagy and mitophagy, a specific type of autophagy for mitochondria [23,47]. This supports that imatinib increased mitochondrial ROS and impaired the mitochondrial membrane potential, which also induces an autophagic response, although we cannot exclude the possibility that other mechanisms, such as inhibition of c-abl-mTOR by imatinib, also induced autophagy [39]. Taken together, imatinib increased mitochondrial ROS and injury, leading to myocyte apoptosis and autophagy at higher clinical doses.

In the present study, imatinib increased the mature autolysosome indicator acridine orange-stained vacuoles and mature cathepsin D expression, in addition to LC3-II and beclin 1expression, which suggests that imatinib induces autophagic degradation. Accumulation of the autophagy indicator LC3-II usually reflects increased autophagy; however, impairment of lysosomal degradation also induces autophagosome accumulation and the increase in LC3-II [36]. In a neuroblastoma cell line, imatinib was previously reported to improve lysosome function and remove intracellular protein aggregates by targeting abl activity [39]. On the other hand, imatinib was reported to impair lysosome function at higher concentrations [48]. Therefore, we examined mature cathepsin D expression as an indicator of lysosomal enzyme activation in the present study and confirmed that imatinib also activated lysosomal enzyme concomitant with the increase in LC3-II. Moreover, in the process of autophagic degradation, acidification of autolysosomes occurs [49] and we confirmed that imatinib also increased acidic mature autolysosomes using acridine orange-staining. Therefore, a clinical dose of imatinib induces autophagic degradation.

Imatinib-induced autophagy is a pro-survival management method against apoptotic cell death because the inhibition of autophagy by 3MA exacerbated imatinib-induced apoptotic cell death *in vitro* and *in vivo*. Two types of autophagy inhibitors are usually used under pathological conditions: inhibitors of autophagosome formation and inhibitors of autolysosome degradation. With these two types of autophagy inhibitors, the latter types cause the accumulation of autophagosomes and Watanabe et al. reported that excessive accumulation of autophagosomes injured cardiac tissue [36]. Therefore, in the present study, to examine the roles of imatinib-induced autophagosome formation and autolysosome degradation in myocyte apoptosis, we selected 3MA as an inhibitor of autophagosome formation instead of autolysosome inhibitors, such as bafilomysin and croloquin, and it exacerbated apoptotic cell death in cultured cardiomyocytes and cardiac tissue. There are several lines of evidence supporting a link between apoptosis and autophagy in cardiac diseases. In ischemic myocardium, pressure overload-induced cardiomyopathy, and septic heart injury, the inhibition of autophagy exacerbates myocyte apoptosis and cardiac function [34,36,50,51]. On the other hand, in cardiomyopathy in patients and animal models, autophagic myocyte death is observed as cellular degeneration [30,37]. Of note, in doxorubicin-induced cardiac toxicity, controversial effects of autophagy were reported; inhibition of autophagy by GATA4 and beclin 1 silence attenuated cardiac injury, and increased autophagy by metformin also attenuated cardiac injury [31,32,52]. A balance between injury of intracellular organelles and levels of autophagy, and inhibition targets in the autophagic pathway may affect the roles of autophagy in pathological conditions. In the present imatinib-induced cardiac injury, autophagy had a pro-survival role to ameliorate mitochondrial apoptosis.

In the present *in vivo* study, imatinib increased apoptosis in association with myocyte hypertrophy, but not interstitial fibrosis, and 3MA increased both of these histological changes. In the failing heart, myocyte hypertrophy and interstitial fibrosis are usually present together, but in the present model, imatinib induced myocyte hypertrophy, but did not increase interstitial fibrosis. Myocyte hypertrophy under imatinib treatment was previously reported and the present study is consistent with these prior studies [7]. Imatinib inhibits the PDGF signaling pathway in addition to bcr-abl tyrosine kinase, and Wang previously reported that imatinib suppressed isoproterenol-induced cardiac fibrosis by inhibiting the PDGF signaling pathway [53]. Therefore, inhibition of this pathway may have affected the interstitial fibrosis in the imatinib-treated heart and co-treatment with 3MA exacerbated cardiac failure, which led to the adverse interstitial fibrosis. Taken together, pro-survival signaling of autophagy attenuated imatinib-induced cardiac histological changes, leading to the preservation of cardiac function.

Cardiotoxicities are important side effects during anti-cancer therapy. In addition to well-known anthracycline-induced cardiac toxicities, those of tyrosine-kinase inhibitors have been recently reported, including imatinib, sorafenib, and sunitunib [6–9,46,54]. These compounds inhibit different kinds of tyrosine-kinases. However, these compounds impair mitochondrial respiration in common, and mitochondrial injury plays a critical role in these compounds-induced cardiac dysfunctions in animal models [54]. Therefore, the present results are consistent with those of prior studies. Cardiomyocytes produce an enormous amount of adenosine triphosphate (ATP) by mitochondria to maintain cardiac contraction and malfunctioning mitochondria cause an impairment of energy metabolism and contractile dysfunction in myocytes. In addition, activation of mitochondrial apoptotic pathway by injured mitochondria leads to myocytes loss and residual myocytes receive mechanical load more, which activates neuro-humoral factors including norepinephrine and angiotensin II and leads to LV dysfunction in association with histological changes, such as myocyte hypertrophy and cardiac fibrosis [44]. Therefore, in the present study imatinib-induced mitochondrial ROS production and associated myocyte loss by apoptosis would exacerbate cardiac dysfunction. In the present model autophagy inhibition would obstruct the removal of injured mitochondria and exacerbate mitochondrial apoptotic pathways. Recent evidence suggests that sirtuin-3, a mitochondrial deacetylase, attenuates doxorubicin-induced mitochondrial impairment by reduction of mitochondrial oxidative stress in cultured H9C2 cells and the overexpression of sirtuin-3 attenuates ventricular dysfunction by amelioration of oxidative stress, suggesting that in the present study autophagy has an endogenous protective pathway to remove malfunctional mitochondria and inhibit apoptosis [55,56].

In conclusion, imatinib induces myocyte mitochondrial injury and apoptosis, leading to cardiac dysfunction. Imatinib also induces myocyte autophagy and autophagy plays a pro-survival role in imatinib-induced cardiotoxicity.

Funding

The present study was supported in part by MEXT/JSPS KAKENHI24591102, Japan.

Author contributions

M.K. and T.N. designed the study. M.K., N.N., and H.T. performed the experiments and analyzed the data. N.N. cared for the animals. M.K. acquired funding. M.K. and T.N. wrote the manuscript. All authors revised and approved the manuscript.

Declaration of Competing Interest

The authors report no declarations of interest.

Acknowledgements

The authors gratefully thank Mihoko Kitamura for her excellent technical assistance with the mouse model.

References

[1] L.A. Torre, F. Bray, R.L. Siegel, J. Ferlay, J. Lortet-Tieulent, A. Jemal, Global cancer statistics, 2012, CA Cancer J. Clin. 265 (2) (2015) 87–108, https://doi.org/10.3322/caac.21262.

[2] K.C. Oeffinger, A.C. Mertens, C.A. Sklar, T. Kawashima, M.M. Hudson, A. T. Meadows, D.L. Friedman, N. Marina, W. Hobbie, N.S. Kadan-Lottick, C. L. Schwartz, W. Leisenring, L.L. Robison, Childhood Cancer Survivor Study, Chronic health conditions in adult survivors of childhood cancer, N. Engl. J. Med. 355 (15) (2006) 1572–1582, https://doi.org/10.1056/NEJMsa060185.

[3] A.Y. Higgins, T.D. O'Halloran, J.D. Chang, Chemotherapy-induced cardiomyopathy, Heart Fail. Rev. 20 (6) (2015) 721–730, https://doi.org/10.1007/s10741-015-9502-y.

[4] L. Jovenaux, J. Cautela, N. Resseguier, M. Pibarot, M. Taouqi, M. Orabona, J. Pinto, M. Peyrol, J. Barraud, M. Laine, L. Bonello, F. Paganelli, F. Barlesi, F. Thuny, Practices in management of cancer treatment-related cardiovascular toxicity: a cardio-oncology survey, Int. J. Cardiol. 241 (2017) 387–392, https://doi.org/10.1016/j.ijcard.2017.02.154.

[5] S. Yamanaka, T. Tatsumi, J. Shiraishi, A. Mano, N. Keira, S. Matoba, J. Asayama, S. Fushiki, H. Fliss, M. Nakagawa, Amlodipine inhibits doxorubicin-induced apoptosis in neonatal rat cardiac myocytes, J. Am. Coll. Cardiol. 41 (March (5)) (2003) 870–878, https://doi.org/10.1016/s0735-1097(02)02935-2.

[6] N. Georgiadis, K. Tsarouhas, R. Rezaee, H. Nepka, G.E.N. Kass, J.L.C.M. Dorne, D. Stagkos, K. Toutouzas, D.A. Spandidos, D. Kouretas, C. Tsitsimpikou, What is considered cardiotoxicity of anthracyclines in animal studies, Oncol. Rep. 44 (3) (2020) 798–818, https://doi.org/10.3892/or.2020.7688.

[7] R. Kerkelä, L. Grazette, R. Yacobi, C. Iliescu, R. Patten, C. Beahm, B. Walters, S. Shevtsov, S. Pesant, F.J. Clubb, A. Rosenzweig, R.N. Salomon, R.A.V. Etten, J. Alroy, J.-B. Durand, T. Force, Cardiotoxicity of the cancer therapeutic agent imatinib mesylate, Nat. Med. 12 (8) (2006) 908–916, https://doi.org/10.1038/nm1446. Epub 2006 Jul 23.

[8] T. Vaidya, J. Kamta, M. Chaar, A. Ande, S. Ait-Oudhia, Systems pharmacological analysis of mitochondrial cardiotoxicity induced by selected tyrosine kinase inhibitors, J. Pharmacokinet. Pharmacodyn. 45 (3) (2018) 401–418, https://doi.org/10.1007/s10928-018-9578-9.

[9] M. Savi, C. Frati, S. Cavalli, G. Graiani, S. Galati, A. Buschini, D. Madeddu, A. Falco, L. Prezioso, G. Mazzaschi, F. Galaverna, C.A.M. Lagrasta, E. Corradini, A. D. Angelis, D. Cappetta, L. Berrino, F. Aversa, F. Quaini, K. Urbanek, Imatinib mesylate-induced cardiomyopathy involves resident cardiac progenitors, Pharmacol. Res. 127 (2018) 15–25, https://doi.org/10.1016/j.phrs.2017.09.020.

[10] M. Deininger, E. Buchdunger, B.J. Druker, The development of imatinib as a therapeutic agent for chronic myeloid leukemia, Blood 105 (7) (2005) 2640–2653, https://doi.org/10.1182/blood-2004-08-3097.

[11] M. Milhem, J.M. Deutsch, Imatinib dosing in gastrointestinal stromal tumors (GISTs): when, how much, and how long? Curr. Clin. Pharmacol. 10 (4) (2015) 311–320, https://doi.org/10.2174/1574884710666151020100518.

[12] B.J. Druker, S. Tamura, E. Buchdunger, S. Ohno, G.M. Segal, S. Fanning, J. Zimmermann, N.B. Lydon, Effects of a selective inhibitor of the Abl tyrosine kinase on the growth of Bcr-Abl positive cells, Nat. Med. 2 (5) (1996) 561–566, https://doi.org/10.1038/nm0596-561.

[13] M.C. Heinrich, D.J. Griffith, B.J. Druker, C.L. Wait, K.A. Ott, A.J. Zigler, Inhibition of c-kit receptor tyrosine kinase activity by STI 571, a selective tyrosine kinase inhibitor, Blood 96 (3) (2000) 925–932.

[14] M. Carroll, S. Ohno-Jones, S. Tamura, E. Buchdunger, J. Zimmermann, N.B. Lydon, D.G. Gilliland, B.J. Druker, CGP 57148, a tyrosine kinase inhibitor, inhibits the growth of cells expressing BCR-ABL, TEL-ABL, and TEL-PDGFR fusion proteins, Blood 90 (12) (1997) 4947–4952.

[15] A.R.G. Francisco, D. Alves, C. David, L. Guerra, F.J. Pinto, A.G. Almeida, Cardiotoxicity in hematological diseases: are the tyrosine kinase inhibitors imatinib and nilotinib safe? Cardiovasc. Toxicol. 18 (5) (2018) 431–435, https://doi.org/10.1007/s12012-018-9453-3.

[16] J.C. Trent, S.S. Patel, J. Zhang, D.M. Araujo, J.-C. Plana, D.J. Lenihan, D. Fan, S. R. Patel, R.S. Benjamin, A.Y. Khakoo, Rare incidence of congestive heart failure in gastrointestinal stromal tumor and other sarcoma patients receiving imatinib mesylate, Cancer 116 (1) (2010) 184–192, https://doi.org/10.1002/cncr.24683.

[17] A.L. Ribeiro, M.S. Marcolino, H.N.S. Bittencourt, M.M. Barbosa, M.C.P. Nunes, V. F. Xavier, N.C.D. Clementino, An evaluation of the cardiotoxicity of imatinib mesylate, Leuk. Res. 32 (12) (2008) 1809–1814, https://doi.org/10.1016/j.leukres.2008.03.020.

[18] H.H. Ran, R. Zhang, X.C. Lu, B. Yang, H. Fan, H.L. Zhu, Imatinib-induced decompensated heart failure in an elderly patient with chronic myeloid leukemia: case report and literature review, J. Geriatr. Cardiol. 9 (4) (2012) 411–414, https://doi.org/10.3724/SP.J.1263.2012.05251.

[19] W. Maharsy, A. Aries, O. Mansour, H. Komati, M. Nemer, Ageing is a risk factor in imatinib mesylate cardiotoxicity, Eur. J. Heart Fail. 16 (4) (2014) 367–376, https://doi.org/10.1002/ejhf.58.

[20] T.P. Chambers, L. Santiesteban, D. Gomez, J.W. Chambers, Sab mediates mitochondrial dysfunction involved in imatinib mesylate-induced cardiotoxicity, Toxicology 382 (2017) 24–35, https://doi.org/10.1016/j.tox.2017.03.006.

[21] K. Takeshige, M. Baba, S. Tsuboi, T. Noda, Y. Ohsumi, Autophagy in yeast demonstrated with proteinase-deficient mutants and conditions for its induction, J. Cell Biol. 119 (2) (1992) 301–311, https://doi.org/10.1083/jcb.119.2.301.

[22] D.J. Klionsky, S.D. Emr, Autophagy as a regulated pathway of cellular degradation, Science 290 (5497) (2000) 1717–1721, https://doi.org/10.1126/science.290.5497.1717.

[23] N. Koleini, E. Kardami, Autophagy and mitophagy in the context of doxorubicin-induced cardiotoxicity, Oncotarget 8 (28) (2017) 46663–46680, https://doi.org/10.18632/oncotarget.16944.

[24] I. Lekli, D.D. Haines, G. Balla, A. Tosaki, Autophagy: an adaptive physiological countermeasure to cellular senescence and ischaemia/reperfusion-associated cardiac arrhythmias, J. Cell. Mol. Med. 21 (6) (2017) 1058–1072, https://doi.org/10.1111/jcmm.13053.

[25] E.H. Baehrecke, Autophagy: dual roles in life and death? Nat. Rev. Mol. Cell Biol. 6 (6) (2005) 505–510, https://doi.org/10.1038/nrm1666.

[26] K. Nishida, O. Yamaguchi, K. Otsu, Crosstalk between autophagy and apoptosis in heart disease, Circ. Res. 103 (4) (2008) 343–351, https://doi.org/10.1161/CIRCRESAHA.108.175448.

[27] J.-O. Pyo, M.-H. Jang, Y.-K. Kwon, H.-J. Lee, J.-I. Jun, H.-N. Woo, D.-H. Cho, B. Choi, H. Lee, J.-H. Kim, N. Mizushima, Y. Oshumi, Y.-K. Jung, Essential roles of Atg5 and FADD in autophagic cell death: dissection of autophagic cell death into vacuole formation and cell death, J. Biol. Chem. 280 (21) (2005) 20722–20729, https://doi.org/10.1074/jbc.M413934200. Epub 2005 Mar 18.

[28] L. Yu, A. Alva, H. Su, P. Dutt, E. Freundt, S. Welsh, E.H. Baehrecke, M.J. Lenardo, Regulation of an ATG7-beclin 1 program of autophagic cell death by caspase-8, Science 304 (5676) (2004) 1500–1502, https://doi.org/10.1126/science.1096645.

[29] Y. Chen, E. McMillan-Ward, J. Kong, S.J. Israels, S.B. Gibson, Mitochondrial electron-transport-chain inhibitors of complexes I and II induce autophagic cell death mediated by reactive oxygen species, J. Cell. Sci. 120 (Pt 23) (2007) 4155–4166, https://doi.org/10.1242/jcs.011163.

[30] H. Akazawa, S. Komazaki, H. Shimomura, Terasaki Fumio, Y. Zou, H. Takano, T. Nagai, I. Komuro, Diphtheria toxin-induced autophagic cardiomyocyte death plays a pathogenic role in mouse model of heart failure, J. Biol. Chem. 279 (September (39)) (2004) 41095–41103, https://doi.org/10.1074/jbc.M313084200. Epub 2004 Jul 22.

[31] S. Kobayashi, P. Volden, D. Timm, K. Mao, X. Xu, Q. Liang, Transcription factor GATA4 inhibits doxorubicin-induced autophagy and cardiomyocyte death, J. Biol. Chem. 285 (1) (2010) 793–804, https://doi.org/10.1074/jbc.M109.070037.

[32] L. Lu, W. Wu, J. Yan, X. Li, H. Yu, X. Yu, Adriamycin-induced autophagic cardiomyocyte death plays a pathogenic role in a rat model of heart failure, Int. J. Cardiol. 134 (1) (2009) 82–90, https://doi.org/10.1016/j.ijcard.2008.01.043.

[33] S. Miyata, G. Takemura, Y. Kawase, Y. Li, H. Okada, R. Maruyama, H. Ushikoshi, M. Esaki, H. Kanamori, L. Li, Y. Misao, A. Tezuka, T. Toyo-Oka, S. Minatoguchi, T. Fujiwara, H. Fujiwara, Autophagic cardiomyocyte death in cardiomyopathic hamsters and its prevention by granulocyte colony-stimulating factor, Am. J. Pathol. 168 (2) (2006) 386–397, https://doi.org/10.2353/ajpath.2006.050137.

[34] Y. Matsui, H. Takagi, X. Qu, M. Abdellatif, H. Sakoda, T. Asano, B. Levine, J. Sadoshima, Distinct roles of autophagy in the heart during ischemia and reperfusion: roles of AMP-activated protein kinase and Beclin 1 in mediating autophagy, Circ. Res. 100 (6) (2007) 914–922, https://doi.org/10.1161/01.RES.0000261924.76669.36.

[35] S. Hein, E. Arnon, S. Kostin, M. Schönburg, A. Elsässer, V. Polyakova, E.P. Bauer, W.-P. Klövekorn, J. Schaper, Progression from compensated hypertrophy to failure in the pressure-overloaded human heart: structural deterioration and compensatory mechanisms, Circulation 107 (7) (2003) 984–991, https://doi.org/10.1161/01.cir.0000051865.66123.b7.

[36] T. Watanabe, G. Takemura, H. Kanamori, K. Goto, A. Tsujimoto, H. Okada, I. Kawamura, A. Ogino, T. Takeyama, T. Kawaguchi, K. Morishita, H. Ushikoshi, M. Kawasaki, A. Mikami, T. Fujiwara, H. Fujiwara, S. Minatoguchi, Restriction of food intake prevents postinfarction heart failure by enhancing autophagy in the surviving cardiomyocytes, Am. J. Pathol. 184 (5) (2014) 1384–1394, https://doi.org/10.1016/j.ajpath.2014.01.011.

[37] M.W. Knaapen, M.J. Davies, M. De Bie, A.J. Haven, W. Martinet, M.M. Kockx, Apoptotic versus autophagic cell death in heart failure, Cardiovasc. Res. 51 (2) (2001) 304–312, https://doi.org/10.1016/s0008-6363(01)00290-5.

[38] M.M. Mocanu, G.F. Baxter, D.M. Yellon, Caspase inhibition and limitation of myocardial infarct size: protection against lethal reperfusion injury, Br. J. Pharmacol. 130 (2) (2000) 197–200, https://doi.org/10.1038/sj.bjp.0703336.

[39] A. Ertmer, V. Huber, S. Gilch, T. Yoshimori, V. Erfle, J. Duyster, H.-P. Elsässer, H. M. Schätzl, The anticancer drug imatinib induces cellular autophagy, Leukemia 21 (5) (2007) 936–942, https://doi.org/10.1038/sj.leu.2404606.

[40] H. Hayashi, M. Kobara, M. Abe, N. Tanaka, E. Gouda, H. Toba, H. Yamada, T. Tatsumi, T. Nakata, H. Matsubara, Aldosterone nongenomically produces NADPH oxidase-dependent reactive oxygen species and induces myocyte apoptosis, Hypertens. Res. 31 (2) (2008) 363–375, https://doi.org/10.1291/hypres.31.363.

[41] E.H. Herman, A. Knapton, E. Rosen, K. Thompson, B. Rosenzweig, J. Estis, S. Agee, Q.-A. Lu, J.A. Todd, S. Lipshultz, B. Hasinoff, J.A. Zhang, Multifaceted evaluation of imatinib-induced cardiotoxicity in the rat, Toxicol. Pathol. 39 (7) (2011) 1091–1106, https://doi.org/10.1177/0192623311419524.

[42] R.A. Larson, B.J. Druker, F. Guilhot, S.G. O'Brien, G.J. Riviere, T. Krahnke, I. Gathmann, Y. Wang, IRIS (International Randomized Interferon vs STI571) Study Group, Imatinib pharmacokinetics and its correlation with response and safety in chronic-phase chronic myeloid leukemia: a subanalysis of the IRIS study, Blood 111 (8) (2008) 4022–4028, https://doi.org/10.1182/blood-2007-10-116475.

[43] A. Wolf, P. Couttet, M. Dong, O. Grenet, M. Heron, U. Junker, U. Laengle, D. Ledieu, E. Marrer, A. Nussher, E. Persohn, F. Pognan, G.J. Rivière, D.R. Roth, C. Trendelenburg, J. Tsao, D. Roman, Imatinib does not induce cardiotoxicity at clinically relevant concentrations in preclinical studies, Leuk. Res. 34 (9) (2010) 1180–1188, https://doi.org/10.1016/j.leukres.2010.01.004.

[44] Kinugawa S. TsutsuiH, S. Matsushima, Mitochondrial oxidative stress and dysfunction in myocardial remodelling, Cardiovasc. Res. 81 (February (3)) (2009) 449–456, https://doi.org/10.1093/cvr/cvn280. Epub 2008 Oct 14.
[45] F.J. Giordano, Oxygen, oxidative stress, hypoxia, and heart failure, J. Clin. Invest. 115 (3) (2005) 500–508, https://doi.org/10.1172/JCI24408.
[46] Y. Will, J.A. Dykens, S. Nadanaciva, B. Hirakawa, J. Jamieson, L.D. Marroquin, J. Hynes, S. Patyna, B.A. Jessen, Effect of the multitargeted tyrosine kinase inhibitors imatinib, dasatinib, sunitinib, and sorafenib on mitochondrial function in isolated rat heart mitochondria and H9c2 cells, Toxicol. Sci. 106 (1) (2008) 153–161, https://doi.org/10.1093/toxsci/kfn157.
[47] J.M. Bravo-San Pedro, G. Kroemer, L. Galluzzi, Autophagy and mitophagy in cardiovascular disease, Circ. Res. 120 (11) (2017) 1812–1824, https://doi.org/10.1161/CIRCRESAHA.117.311082.
[48] G. Yogalingam, A.M. Pendergast, Abl kinases regulate autophagy by promoting the trafficking and function of lysosomal components, J. Biol. Chem. 283 (51) (2008) 35941–35953, https://doi.org/10.1074/jbc.M804543200.
[49] I. Papandreou, A.L. Lim, K. Laderoute, N.C. Denko, Hypoxia signals autophagy in tumor cells via AMPK activity, independent of HIF-1, BNIP3, and BNIP3L, Cell Death Differ. 15 (10) (2008) 1572–1581, https://doi.org/10.1038/cdd.2008.84.
[50] Y. Sun, X. Yao, Q.J. Zhang, M. Zhu, Z.P. Liu, B. Ci, Y. Xie, D. Carlson, B. A. Rothermel, Y. Sun, B. Levine, J.A. Hill, S.E. Wolf, J.P. Minei, Q.S. Zang, Beclin-1-dependent autophagy protects the heart during sepsis, Circulation 138 (20) (2018) 2247–2262, https://doi.org/10.1161/CIRCULATIONAHA.117.032821.
[51] A. Nakai, O. Yamaguchi, T. Takeda, Y. Higuchi, S. Hikoso, M. Taniike, S. Omiya, I. Mizote, Y. Matsumura, M. Asahi, K. Nishida, M. Hori, N. Mizushima, K. Otsu, The role of autophagy in cardiomyocytes in the basal state and in response to hemodynamic stress, Nat. Med. 13 (5) (2007) 619–624, https://doi.org/10.1038/nm1574.
[52] R. Zilinyi, A. Czompa, A. Czegledi, A. Gajtko, D. Pituk, I. Lekli, A. Tosaki, The cardioprotective effect of metformin in doxorubicin-induced cardiotoxicity: the role of autophagy, Molecules. 23 (5) (2018) 1184, https://doi.org/10.3390/molecules23051184.
[53] L.-X. Wang, X. Yang, Y. Yue, T. Fan, J. Ho, G.-X. Chen, M.-Y. Liang, Z.-K. Wu, Imatinib attenuates cardiac fibrosis by inhibiting platelet-derived growth factor receptors activation in isoproterenol induced model, PLoS One 12 (June (6)) (2017), e0178619, https://doi.org/10.1371/journal.pone.0178619.
[54] Z.V. Varga, P. Ferdinandy, L. Liaudet, P. Pacher, Drug-induced mitochondrial dysfunction and cardiotoxicity, Am. J. Physiol. Heart Circ. Physiol. 309 (9) (2015) H1453–H1467, https://doi.org/10.1152/ajpheart.00554.2015.
[55] K.G. Cheung, L.K. Cole, B. Xiang, K. Chen, X. Ma, Y. Myal, G.M. Hatch, Q. Tong, V. W. Dolinsky, Sirtuin-3 (SIRT3) protein attenuates doxorubicin-induced oxidative stress and improves mitochondrial respiration in H9c2 cardiomyocytes, J. Biol. Chem. 290 (17) (2015) 10981–10993, https://doi.org/10.1074/jbc.M114.607960.
[56] Q. Du, B. Zhu, Q. Zhai, B. Yu, Sirt3 attenuates doxorubicin-induced cardiac hypertrophy and mitochondrial dysfunction via suppression of Bnip3, Am. J. Transl. Res. 9 (7) (2017) 3360–3373.